Desalination and Water Treatment
www.deswater.com

doi: 10.5004/dwt.2019.24860

172 (2019) 270–280
December

Evaluation of electro-Fenton method on cheese whey treatment: optimization through response surface methodology

Ş. Camcıoğlu, B. Özyurt*, S. Şengül, H. Hapoğlu

Faculty of Engineering Department of Chemical Engineering, Ankara University, Tandoğan, Ankara, Turkey, emails: bozyurt@ankara.edu.tr (B. Özyurt), camcioglu@eng.ankara.edu.tr (Ş. Camcıoğlu), seliinsengul@gmail.com (S. Şengül), hapoglu@eng.ankara.edu.tr (H. Hapoğlu)

Received 1 April 2019; Accepted 4 September 2019

ABSTRACT

In this study, the efficiency of real cheese whey treatment using a low-cost graphite-graphite electro-Fenton (EF) method and the effects of operating parameters on the process were investigated using central composite design. Response surface methodology was used to evaluate the effect of process variables and their interaction on chemical oxygen demand (COD) removal, energy consumption, and current efficiency. Results show that selected operational parameters and obtained regression models were statistically significant. The coefficient of determination of COD removal, energy consumption, and current efficiency were found as 0.9884, 0.9371, and 0.8479, respectively, indicating that the models have a good fits with experimental data. Optimum operating conditions were determined as 0.0625 mol $FeSO_4·7H_2O$, 14.48 $H_2O_2/FeSO_4·7H_2O$ molar ratio and 1.22 A current intensity (9.68 mA/cm^2 current density). EF treatment study under optimal conditions yielded 86.75% COD removal and 0.36 kWh/kg COD_r energy consumption with 47.11% current efficiency. The results show that the present treatment with the use of low-cost graphite electrodes yielded highly competitive and promising results under low current density conditions.

Keywords: Cheese whey wastewater; Electro-Fenton; Response surface methodology; Central composite design; Graphite electrode

1. Introduction

Cheese whey is the yellowish-green liquid which is obtained by the separation of casein and fat from the milk by coagulation during the cheese-making process. This by-product represents about 80%–90% of the total volume of milk used in cheese production containing lactose (4.5%–5% w/v), soluble proteins (0.6%–0.8% w/v), lipids (0.4%–0.5% w/v), lactic acid (0.05% w/v) and mineral salts (8%–10% of dried extract) [1,2]. In large scale plants, it is possible to process cheese whey through valorization technologies to recover protein and lactose or to dry and use as feedstock for animal feeding [3,4]. However, in individual small-scale dairy farms or cheese production facilities, whey is not recovered and must be treated with other wastewater produced from the plant, because the small amount produced does not meet the high equipment cost required for the preparation of whey powder [4]. On the other hand, as a wastewater, lactose content of influent is largely responsible for the high biochemical and chemical oxygen demand (BOD and COD) values, concurrently fats and proteins partially contribute as well [5]. The high content of biodegradable organic material can cause rapid oxygen consumption, impermeabilization, eutrophication and toxicity in the receiving environments which results in water quality degradation [5,6]. Cheese whey disposal has become a significant environmental impact due to the

* Corresponding author.

Presented at the 4th International Conference on Recycling and Reuse 2018 (R&R2018), 24–26 October 2018, Istanbul, Turkey

1944-3994/1944-3986 © 2019 Desalination Publications. All rights reserved.

high production amount and heavy organic pollutant load. More stringent legislative requirements for effluent quality necessitate treatment before discharge [3].

Various treatment processes have been developed for cheese whey removal from water, including anaerobic biological treatment [7], adsorption [8], coagulation [9] and Fenton oxidation [10]. Since the BOD/COD ratio is higher than 0.5, biological processes are very effective in organic matter removal from cheese whey [5]. However, there are some drawbacks of biological treatment such as long hydraulic retention times to observe satisfactory performance, the necessity of specific microorganisms, sludge floatation because of the presence of fats and unstable operation [6,11]. Physicochemical treatment such as coagulation and adsorption only transfers the contaminants between different phases. Chemical methods such as Fenton oxidation is capable of destroying the pollutants and eventually resulting in high COD removal efficiencies from cheese whey [12]. Electrochemical advanced oxidation processes (EAOPs), which are known as eco-friendly methods, are receiving great attention as a viable and promising alternative to degrade the refractory organic pollutants due to generation of hydroxyl radicals on-site [12]. Electrochemical methods utilize only electrons to assist wastewater treatment with the purpose of controlled and rapid reactions instead of chemicals and microorganisms [13]. Moreover, the sludge that is generated by electrochemical systems is defined as easily settleable and predominantly composed of metal oxides/hydroxides [13].

Electro-Fenton (EF) process which is the most known and popular EAOP based on Fenton's reaction chemistry, has two different configurations. The first configuration involves the addition of Fenton reagents to the reactor from outside and the utilization of inert electrodes with high catalytic activity as an anode. In the second one, only hydrogen peroxide is added from outside whereas Fe^{2+} is provided from sacrificial iron anodes [14]. Ferrous ions may either be produced via oxidative dissolution of sacrificial anodes (Eq. (1)) or by reduction of ferric ions at an inert cathode (Eq. (2)) [15].

$$Fe^0 \rightarrow Fe^{2+} + 2e^- \quad (1)$$

$$Fe^{3+} + e^- \rightarrow Fe^{2+} \quad (2)$$

If the ferrous ions are added externally, anode materials like Pt, boron-doped diamond, graphite can be used in EF studies [16]. These materials lead to the water oxidation and hydroxyl radicals are produced at the surface of a high oxygen overvoltage anode (Eq. (3)) which will assist organic pollutant removal [16]. At anode surface, oxygen evolution reaction also occurs as given in Eq. (4) which reduces current efficiency. Graphite, among others, stands out as an alternative EF electrode material because of its low cost [16].

$$H_2O \rightarrow HO^{\bullet} + H^+ + e^- \quad (3)$$

$$2H_2O \rightarrow 4H^+ + O_2 + 2e^- \quad (4)$$

The electrochemical reduction of oxygen in the two- or the four-electron process occurs on the cathode [17]. H_2O_2 is electrogenerated in acidic solutions by two-electron reduction of oxygen on the cathode surface according to Eq. (5) depending on the cathode material [16].

$$O_2 + 2H^+ + 2e^- \rightarrow H_2O_2 \quad (5)$$

Hydroxyl radicals production can also take place in solution bulk under electrochemically assisted Fenton's reaction (Eq. (6)) [18]. Hydroxyl radical is one of the most reactive free radical that can easily degrade organic materials, and ensure high reactivity and strong non-selective oxidation by in situ production [19,20].

$$Fe^{2+} + H_2O_2 \rightarrow Fe^{3+} + OH^- + HO^{\bullet} \quad (6)$$

The degradation mechanism of organic pollutants by Fenton reaction is given in Eqs. (7) and (8), where RH denotes organic pollutants [14].

$$RH + HO^{\bullet} \rightarrow R^{\bullet} + H_2O \quad (7)$$

$$RH + HO^{\bullet} \rightarrow ROH + \frac{1}{2}H_2 \quad (8)$$

The catalytic Fenton's reaction (Eq. (6)) is propagated from Fe^{2+} regeneration, which takes place by reduction of Fe^{3+} species at the cathode, with H_2O_2, with organic radical intermediates $R^{\bullet}$, and/or with hydroperoxyl radical ($HO_2^{\bullet}$) [21].

The ranges of some operational parameters and treatment performance results for electrochemical and Fenton based treatment of cheese whey in the previously published work were compared with the present study in Table 1. Tezcan Un et al. [1] examined continuous electrocoagulation (EC) treatment of cheese whey wastewater and results showed that 86.4% COD removal was achieved in 20 min under high current density condition. Güven et al. [3] studied cheese whey wastewater treatment using the EC process and after an excessive treatment time of 8 h, the highest COD removal was obtained as 53.32%. Vlyssides et al. [4] applied Fenton treatment to cheese making factory wastewater and found 33% total organic carbon removal in 1 h with a higher $FeSO_4{\cdot}7H_2O/H_2O_2$ ratio. Tezcan Un et al. [22] investigated the EC treatment of whey wastewater using iron anode. The effect of EF by the addition of H_2O_2 was also determined in this study. 90.92% COD removal and 10.60 kWh/kg COD_r energy consumption were observed in 90 min of treatment under optimum conditions of pH 3, a high current density of 40 mA/cm^2 with the addition of 0.2 M Na_2SO_4 and 0.2 M H_2O_2.

Tirado et al. [12] emphasized the need for more electrochemical cheese whey wastewater treatment studies to be able to clarify its feasibility. This work is focused on examining the efficiency of real cheese whey treatment using the EF method and the effects of operating parameters on the process were investigated via central composite design (CCD). Statistical models were developed between the amount of $FeSO_4{\cdot}7H_2O$ added, $H_2O_2/FeSO_4{\cdot}7H_2O$ molar ratio and current intensity as factors, and COD removal, energy consumption, and current efficiency as responses. Optimization of operational parameters with the multi objectives of

Table 1
Comparison of parameters and results for various treatment methods of cheese whey

Reference	Method	Parameters	Ranges for parameters	Optimum conditions	Results
[1]	EC	Current density (mA/cm^2)	40–60	60	COD removal: 86.4%
		pH	3–7	4.54	
		Retention time (min)	20–60	20	
[3]	EC	Waste concentration (%)	20–100	60	COD removal: 53.32% in 8 h
		Applied voltage (V)	2–12	12	
		Electrolyte concentration (g/L)	0–50	25	
[4]	Fenton	$FeSO_4·7H_2O/H_2O_2$	2/3–4/3	2/3	TOC removal: 33%
		Hydraulic retention time (h)	1–5	1	
		pH	3.4–4.2	3.4	
		Temperature (°C)	20–30	20	
[22]	EC	Current density (mA/cm^2)	30–40	40	COD removal: 90.92% in 90 min
		pH	3–9	3	
		Supporting electrolyte type	$NaNO_3$, KNO_3, KCl, NaCl, Na_2SO_4, K_2SO_4	Na_2SO_4	Energy consumption: 10.60 kWh/kg COD_r
		Supporting electrolyte concentration (M)	0.1–0.2	0.2	
The present study	EF	$FeSO_4·7H_2O$ (mol)	0.007–0.065	0.0625	COD removal: 86.75% in 60 min
		$H_2O_2/FeSO_4·7H_2O$	3.3–14.7	14.48	
		Current intensity (A)	0.46–4.54	1.22	Energy consumption: 0.36 kWh/kg COD_r Current efficiency: 47.11%

maximum pollutant removal at the highest current efficiency and minimum energy intake were performed.

2. Materials and methods

2.1. Wastewater

Cheese whey used in this study was obtained from a dairy products plant located in Turkey. Characterization of cheese whey is presented in Table 2. The wastewater was kept in a refrigerator at 4°C before use in order to avoid degradation.

Table 2
Characteristics of real cheese whey

Parameters	Values
pH	5.03
Electrical conductivity, mS/cm	1.70
Turbidity, NTU	9.78 ± 0.5
COD, mg/L	19,800 ± 200

2.2. Experimental setup and procedure

Commercial graphite plate was obtained from a local supplier (Haksan Industrial Materials, Turkey) with specifications of 12.01 g/mol molecular weight, 1.8 g/cm^3 apparent density, 12 μΩ/m specific resistance, 60 mPa compression strength, 0.05% ash, 0.05% sulphur, 25 μm grain size and 15% apparent porosity. Experiments were carried out in a batch 2 L glass reactor with monopolar parallel-connected six graphite electrodes having dimensions of 7 cm × 10 cm × 0.3 cm. In each run, 1 L of cheese whey was fed to the reactor. A direct current power supply (Marxlow PS 305 D, China) operating in 0–2 A range was utilized to perform the experiments at constant current intensity. Uniform concentration dispersion in the reactor was maintained by a magnetic stirrer (MTOPS MS300HS) operating at a prespecified speed of 600 rpm. The experimental system is presented in Fig. 1.

Many studies evidenced that pH 3 assures ideal conditions to optimize the electrochemical production of hydrogen peroxide according to the Eq. (5) and favor the removal of oxidizable organic matter in EF processes [23–27]. In each experimental run, the initial pH value of cheese whey was adjusted to 3 using 10% H_2SO_4 (w/w). Increasing the total dissolved solids concentration of the treated wastewater reduces the water quality in the receiving environment, and various regulatory authorities impose strict limitations on it. Various studies reported the use of NaCl as supporting electrolyte within the concentration range of 1–2 g/L is appropriate for organics removal from wastewater using electrochemical methods [28–31]. Accordingly, 1.5 g NaCl was added to maintain a conductive medium. 50% H_2O_2 (w/w) and $FeSO_4·7H_2O$ were added to the reactor in conformity with their relative ratio in the experimental design matrix. The current intensity was set to the values specified in the design matrix and 60 min of EF treatment was started. At the end of the run pH of the wastewater was adjusted to 8 to provide the removal of other pollutants by coagulation and sedimentation as well as Fe^{3+} ions using 2 M $Ca(OH)_2$ solution. $Ca(OH)_2$ was considered as the most effective of the bases

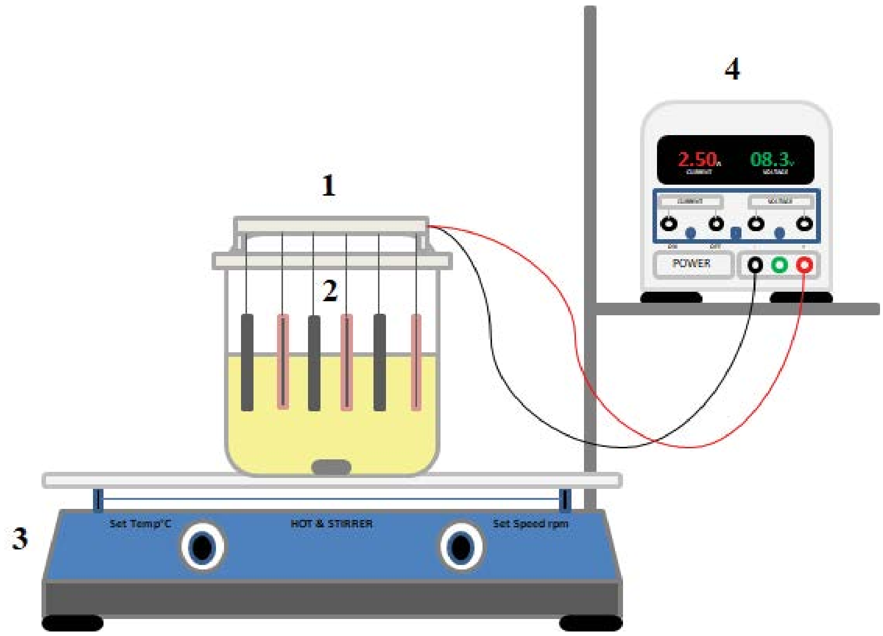

Fig. 1. Experimental system (1: EF reactor, 2: electrodes, 3: magnetic stirrer, and 4: power supply).

commonly used by several studies [32–35]. In the alkaline $Ca(OH)_2$ solution, Fe^{3+} forms highly insoluble $Fe(OH)_3$ ($K_{sp} = 10^{-36}$) in equilibrium with FeO(OH), to give a flocculant precipitate which facilitates the separation of suspended materials in effluent [32,33]. The charge neutralization effect of the coagulants was increased by the presence of $Ca(OH)_2$ at neutral and alkaline pH [35]. 50 ml sample was taken and kept at 4°C for 6 h to settle. COD analyses were performed on collected supernatant by Standard Methods (SM 5220D) twice with ±2% accuracy [36]. Sample storage and settling conditions were chosen by considering SM 5220 D in which maximum sample holding time is 28 d at 4°C accordingly with the studies reported by Lai and Lin [37] and Özyurt et al. [38]. To determine COD values, the absorbance of the samples was read at 600 nm using a spectrophotometer (PG Instruments T60V, United Kingdom). Impurities accumulated on the electrode surfaces were removed at the end of each experiment according to the electrode cleaning procedure by the steps of brushing under tap water, immersing in 5% HCl solution for 5 min and then rinsing with deionized water. Voltage-time data were collected during treatment and energy consumption values per kg of COD removed were calculated considering Eq. (9) where I is the applied constant current intensity in A, V_m is the mean potential difference in V, t is the treatment time in h, COD_i and COD_t are the initial and final COD values of cheese whey in mg/L and V_E is the volume of wastewater in L.

$$\text{Energy consumption}\left(\frac{\text{kWh}}{\text{kg COD}_r}\right) = \frac{I \times V_m \times t \times 1000}{\left(\text{COD}_i - \text{COD}_t\right) \times V_E} \quad (9)$$

Current efficiency that was used to assess the influence of current intensity on organic pollutant removal was calculated using Eq. (10) [38]. Here, F represents the Faraday constant (96,485 C/mol).

$$\text{Current efficiency}\left(\%\right) = \frac{\left(\text{COD}_i - \text{COD}_t\right) \times F \times V_E}{3600 \times 1000 \times 8 \times I \times t} \quad (10)$$

2.3. Experimental design

In this study, CCD was applied to investigate the main variables affecting EF treatment of cheese whey, as well as their interactions. MINITAB 17 software was employed for experimental design, modeling, data analysis, and optimization. $FeSO_4 \cdot 7H_2O$ molar amount, $H_2O_2/FeSO_4 \cdot 7H_2O$ molar ratio and current intensity were chosen as factors, whereas COD removal, energy consumption, and current efficiency were considered as responses. Each of the factors was coded at five levels (−2, −1, 0, +1, +2) and coded values along with the real ones are given in Table 3 where the maximum and minimum values of parameters were chosen by considering the raw cheese whey characteristics. A total of 20 experiments with 8 factorial, 6 axial and 6 central points were performed.

Experimental results were fitted to quadratic response surface models that are generally shown as in Eq. (11) [39].

$$y = \beta_0 + \sum_{j=1}^{k} \beta_j x_j + \sum_{i<j} \beta_{ij} x_i x_j + \sum_{j=1}^{k} \beta_{jj} x_j^2 + \in \quad (11)$$

Analysis of variance (ANOVA) was used to determine the statistical significance of the quadratic models and model terms using the F-test and corresponding P values. The F value of the model should be higher than that of the F distribution table value provided that the best fit of the experimental data with the model is desired. To indicate if the F value is large enough to imply the statistical significance, P-value related to the F value was used. P values lower than 0.05 at 95% confidence level refers to the significance

Table 3
Coded and real values of independent variables for EF treatment of cheese whey

Level	Factors		
	x_1	x_2	x_3
	$FeSO_4·7H_2O$ (mol)	$H_2O_2/FeSO_4·7H_2O$	Current intensity (A)
–2	0.007	3.3	0.46
–1	0.018	5.5	1.25
0	0.036	9.0	2.50
+1	0.054	12.5	3.75
+2	0.065	14.7	4.54

of model and model terms [39]. Besides, to check the accuracy of the proposed quadratic models, determination coefficients (R^2) between experimental and predicted results were evaluated. R^2 represents the correlation of total variation in the responses (COD removal, energy consumption, current efficiency) estimated by suggested models. R^2 values should be at least 0.80 to imply quadratic fits expressing the design space are satisfactory [13]. 3D response surface plots which were constructed as a function of two independent variables varying within the experimental range while the other variables kept constant at the central level, visually displayed the changes in responses to variations of independent variables [39]. Response surfaces were analyzed to obtain the maximum COD removal and current efficiency with minimum energy consumption responses and the corresponding optimum conditions.

3. Results

The experimental design matrix showing combinations of 3 independent variables at 5 levels and obtained responses are represented in Table 4. Experimental results were fitted to statistically significant second-order multi-variable models to indicate the main and interaction effects of the factors on responses. The effect of each variable on the predicted responses was visualized based on the model equation by three dimensional (3D) and contour (2D) plots.

3.1. Model development, statistical analysis and effects of factors on responses

3.1.1. COD removal

The quadratic model that describes the variations in COD removal with operational parameters in terms of uncoded variables was developed and shown in Eq. (12).

$$\text{COD removal}(\%) = -21.56 + 1525x_1 + 4.19x_2 + 0.247x_3 - 11166x_1^2 - 0.1150x_2^2 + 28.3x_1x_2 \quad (12)$$

Table 4
Experimental design matrix and responses for EF treatment of cheese whey

Run	Factors			Responses		
	x_1	x_2	x_3	y_1	y_2	y_3
	$FeSO_4·7H_2O$ (mol)	$H_2O_2/FeSO_4·7H_2O$	Current intensity (A)	COD removal (%)	Energy consumption (kWh/kg COD_r)	Current efficiency (%)
1	0.036	3.3	2.50	32.67	2.99	8.56
2	0.036	14.7	2.50	73.91	1.21	19.01
3	0.036	9.0	2.50	59.91	1.84	16.04
4	0.036	9.0	2.50	54.77	1.57	15.24
5	0.018	5.5	1.25	25.33	1.73	13.44
6	0.036	9.0	2.50	57.64	1.89	15.72
7	0.018	12.5	3.75	41.92	4.83	7.21
8	0.054	12.5	3.75	80.63	2.00	14.07
9	0.036	9.0	0.46	54.80	0.12	78.19
10	0.036	9.0	2.50	55.99	1.73	14.70
11	0.054	5.5	3.75	56.49	3.21	10.04
12	0.036	9.0	2.50	57.81	1.35	15.13
13	0.054	12.5	1.25	80.70	0.34	45.05
14	0.036	9.0	2.50	57.75	1.57	15.96
15	0.018	12.5	1.25	44.68	0.70	23.43
16	0.036	9.0	4.54	57.91	3.80	8.34
17	0.007	9.0	2.50	17.09	6.23	4.48
18	0.018	5.5	3.75	28.76	5.36	5.11
19	0.054	5.5	1.25	58.05	0.56	30.35
20	0.065	9.0	2.50	77.71	1.05	20.83

The COD removal model was statistically analyzed by applying the *F* test to verify the significance of the model and model terms. ANOVA results are given in Table 5. It can be concluded from Table 5 that the *F* value of 201.88 reveals the statistical significance of the COD removal model compared with the tabulated *F* value ($F_{0.05(6,13)}$ = 2.92). From ANOVA results it is clear that linear, square and interaction terms of $FeSO_4·7H_2O$ molar amount and $H_2O_2/FeSO_4·7H_2O$ molar ratio have *P* values lower than 0.05 were significant terms for COD removal of cheese whey treated by EF method. A comparison of actual and predicted COD removal values was visualized in Fig. 2a. R^2 was found as 0.9884 indicating that experimental results are in good fit with predicted data and only 1.16% of the total variation could not be explained by the developed model for COD removal. R^2 value should be compared with $R^2_{adjusted}$ which reflects the number of factors in the experiment. When R^2 and $R^2_{adjusted}$ values are close, there is a good chance that non-significant terms have not been included in the model [39,40]. $R^2_{adjusted}$ value was found very close to R^2, which is another good indicator of the statistical significance of the terms included in the model. $R^2_{predicted}$ which describes the prediction capability of the model for new responses, should not have a difference of more than 0.2 with R^2 [40]. The difference between R^2 and $R^2_{predicted}$ value was found small enough to maintain the predictive capability of the model. Response surface and contour graphs were produced via the developed model equations by keeping one of the factors constant at the central level and varying the other two variables within the experimental design space. Response surface plots of COD removal were shown in Fig. 3a. As can be observed, $FeSO_4·7H_2O$ molar amount and $H_2O_2/FeSO_4·7H_2O$ molar ratio had a significant influence on COD removal whereas current intensity was not. COD removal was increased with increasing x_1 and x_2. Therefore, maximum COD removal efficiency was obtained at a high $FeSO_4·7H_2O$ molar amount and $H_2O_2/FeSO_4·7H_2O$ molar ratio.

The increase in COD removal efficiency with the increase in ferric ion concentration was mainly due to the increase in the in situ generation rate of hydroxyl radical [41].

Iron and hydrogen peroxide are two basic reagents that play a major role in pollutant removal efficiency and operating cost in the EF method. The number of chemicals required must also be evaluated in terms of both the absolute concentration of reagents (i.e. hydrogen peroxide and ferrous ions) and their molar ratio ($H_2O_2/FeSO_4·7H_2O$). Although

Table 5
ANOVA results of COD removal for EF treatment of cheese whey

Source	*df*	SS_{adj}	MS_{adj}	*F*	*P*	Remark
Model	6	5,944.29	990.72	201.88	≤0.0001	Very significant
x_1	1	4112.74	4112.74	838.08	≤0.0001	Very significant
x_2	1	1612.85	1612.85	328.66	≤0.0001	Very significant
x_3	1	1.27	1.27	0.26	0.619	Not significant
x_1^2	1	173.75	173.75	35.41	≤0.0001	Very significant
x_2^2	1	26.36	26.36	5.37	0.037	Significant
x_1x_2	1	25.49	25.49	5.19	0.040	Significant
Error	13	63.80	4.91			
Total	19	6008.09				
R^2 = 0.9884, $R^2_{adjusted}$ = 0.9845, $R^2_{predicted}$ = 0.9654						

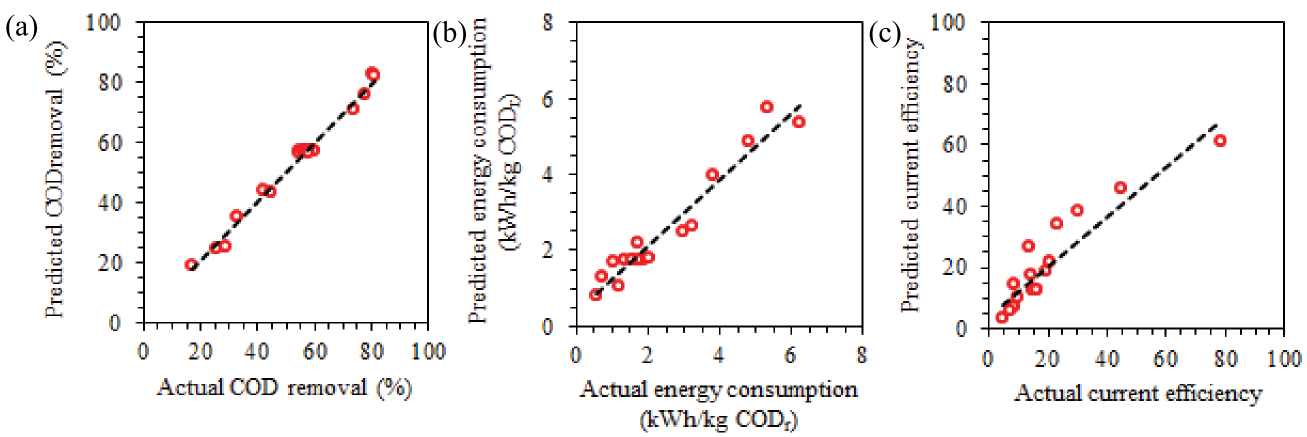

Fig. 2. Actual vs. predicted plots of (a) COD removal, (b) energy consumption, and (c) current efficiency for EF treatment of cheese whey.

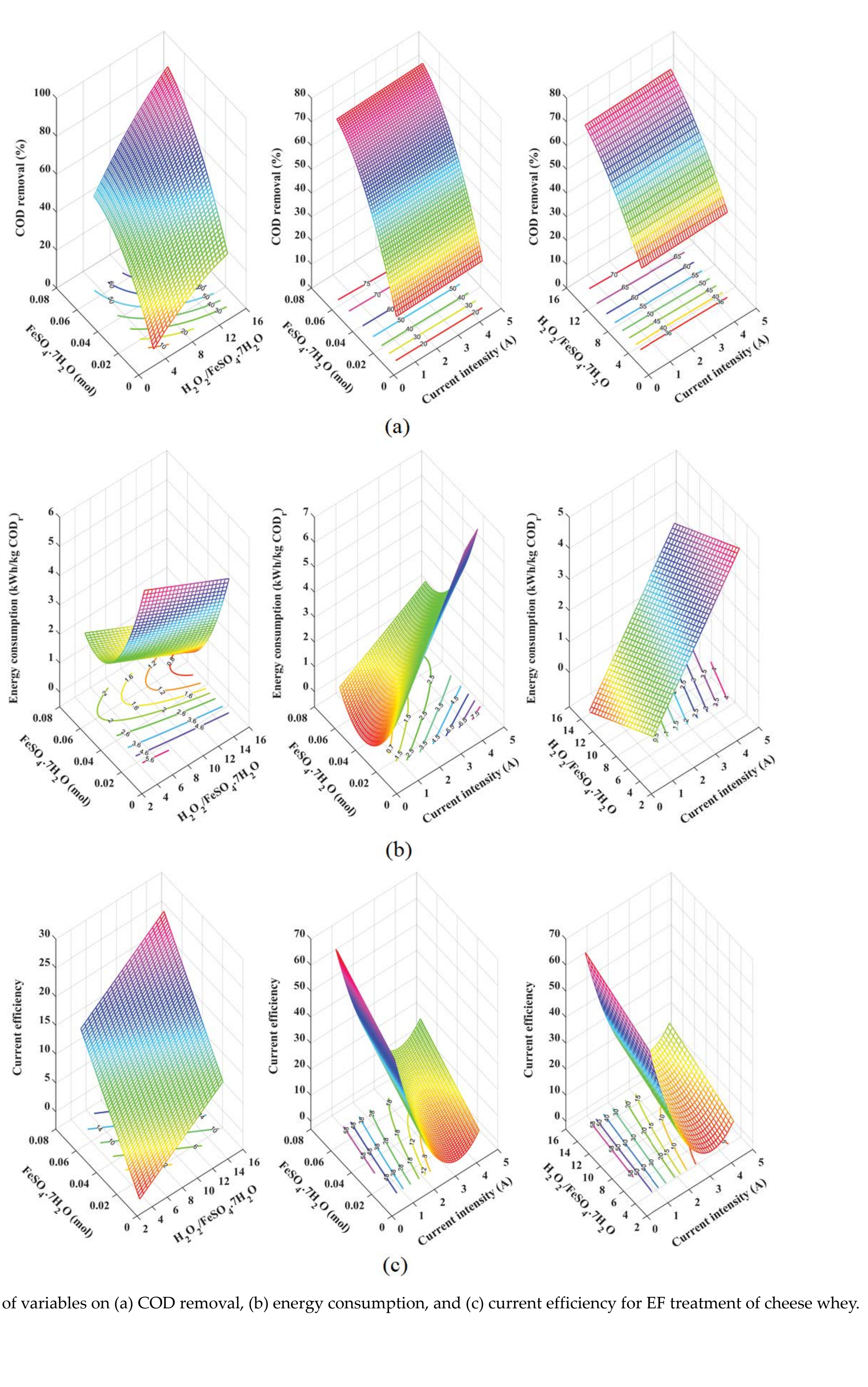

Fig. 3. Effect of variables on (a) COD removal, (b) energy consumption, and (c) current efficiency for EF treatment of cheese whey.

the removal of organic contaminants was improved as the concentration of reagents increases, it was observed that the change in the removal efficiency becomes insignificant when the dosage exceeds the threshold level. Excessive application of iron can promote an increase in the total dissolved solids and electrical conductivity of the effluent while an excessive dosage of hydrogen peroxide contributes to the generation of gas bubbles that prevents sludge settling [42]. Thus, it is important to determine the absolute optimal concentration of Fenton reagents. Increments in COD removal efficiency with increasing $H_2O_2/FeSO_4{\cdot}7H_2O$ molar ratio can be attributed to running the Fenton reaction in the reactor, subsequent formation of highly reactive hydroxyl radical that oxidize the organic contaminants and hence increased rate of oxidation [43,44].

Although current intensity controls the dissolution and regeneration of Fe^{2+} and electro generation of H_2O_2, Fenton reaction in the reactor when no current was applied between the electrodes highly contributes to COD removal and therefore the effect of current intensity on oxidation efficiency was seemed to be diminished [43,45]. The application of current intensity above a certain value reduces both the current efficiency by increasing the oxygen evolution reaction rate and also causes the excess electron generation of iron ion to deplete the hydroxyl radicals, which may hurt the COD removal efficiency [46].

3.1.2. Energy consumption

Experimental results were fitted to a second-order model to examine the effects of independent variables on energy consumption and given by Eq. (13).

$$\text{Energy consumption}\left(\frac{\text{kWh}}{\text{kg COD}_r}\right) = 3.339 - 160.4x_1 - 0.1264x_2 + 1.775x_3 + 2027x_1^2 - 19.17x_1x_3 \quad (13)$$

Statistical significance of the model was investigated through the F test at a 95% confidence level. ANOVA results for energy consumption presented in Table 6 indicate that the F value of 41.74 was found to be higher than the F distribution table value ($F_{0.05(5,14)} = 2.96$) expressing the statistical significance of the developed model. Also, linear terms of all independent variables, the square term of $FeSO_4{\cdot}7H_2O$ molar amount and an interaction term between $FeSO_4{\cdot}7H_2O$ molar amount and current intensity were evaluated as significant according to P values. The actual and predicted results comparison of energy consumption is given in Fig. 2b. The R^2 value was determined to be 0.9371 confirming the good agreement between the experimental data and predicted results from the model. R^2_{adjusted} value was found very close to R^2, which is another good indicator of the statistical significance of the terms included in the model. The difference between R^2 and $R^2_{\text{predicted}}$ value was found small enough to maintain the predictive capability of the model. The influence of operational parameters on energy consumption was demonstrated in Fig. 3b. It is clear from the figure that all factors have significant effects on the response. As seen from the figure, an energy consumption decrease was observed for $FeSO_4{\cdot}7H_2O$ molar amount in the range of 0.007–0.04 mol. Besides, $FeSO_4{\cdot}7H_2O$ molar amount higher than 0.04 mol caused a slight increase in energy consumption. It can be concluded from the figure that energy consumption decreases with an increase in $H_2O_2/FeSO_4{\cdot}7H_2O$ molar ratio and a decrease in current intensity. The optimum value for minimum energy consumption was obtained in the region of a high level - midpoint region for $FeSO_4{\cdot}7H_2O$ molar amount, in the high levels of $H_2O_2/FeSO_4{\cdot}7H_2O$ molar ratio and the low levels of current intensity, respectively.

Since Fe^{2+} ion required for Fenton reaction could not be provided at low concentrations of $FeSO_4{\cdot}7H_2O$, COD removal efficiency reduces and energy consumption per kg COD removed increases accordingly.

An increase in $H_2O_2/FeSO_4{\cdot}7H_2O$ molar ratio leads to a reduction in the conductivity of the effluent, thus increasing the potential difference required to maintain the constant current condition and in consequence results in high energy consumption per volume of wastewater. However, the increase in COD removal efficiency observed with the increase in $H_2O_2/FeSO_4{\cdot}7H_2O$ molar ratio is more significant than the effect of conductivity and resulted in decreased energy consumption per kg COD removed. Consequently, optimization of the $H_2O_2/FeSO_4{\cdot}7H_2O$ molar ratio is essential for an energy-efficient treatment as well as pollutant removal.

Table 6
ANOVA results of energy consumption for EF treatment of cheese whey

Source	*df*	SS_{adj}	MS_{adj}	F	P	Remark
Model	5	51.1666	10.2333	41.74	≤0.0001	Very significant
x_1	1	16.8051	16.8051	68.54	≤0.0001	Very significant
x_2	1	2.6079	2.6079	10.64	0.006	Significant
x_3	1	24.5149	24.5149	99.98	≤0.0001	Very significant
x_1^2	1	5.7509	5.7509	23.46	≤0.0001	Very significant
x_1x_3	1	1.4878	1.4878	6.07	0.027	Significant
Error	14	3.4327	0.2452			
Total	19	54.5993				

$R^2 = 0.9371$, $R^2_{\text{adjusted}} = 0.9147$, $R^2_{\text{predicted}} = 0.7945$

It is well known that the current intensity increases with the applied voltage. Therefore, it is necessary to limit the current intensity to avoid excessive heat generation and high energy consumption.

3.1.3. Current efficiency

Regression equation in terms of uncoded variables obtained for estimating current efficiency based on experimental design results is presented as follows:

$$\text{Current efficiency} = 58.1 + 321x_1 + 1.026x_2 + 41.52x_3 + 6.02x_3^2 \quad (14)$$

The adequacy of the model was evaluated through ANOVA and has shown in Table 7. Results indicated that the quadratic model having an *F*-value of 20.90 which is greater than tabulated *F* ($F_{0.05(4,15)}$ = 3.06) and a *P* value of 0.000 which is below 0.05 at 95% confidence level for current efficiency can be used to navigate the design space. According to Table 7, the independent variables that have a significant individual effect on current efficiency were found as $FeSO_4·7H_2O$ molar amount and current intensity which also has a significant quadratic effect. Fig. 2c is a comparison of actual and predicted current efficiency and implies a good agreement between the results. The R^2 value was determined as 0.8479, expressing that the model represents the experimental data acceptably. $R^2_{adjusted}$ value was found close to R^2, which is another good indicator of the statistical significance of the terms included in the model. The difference between R^2 and $R^2_{predicted}$ value was not found small enough to maintain the predictive capability of the model. The predicted contour plots with the 3D representations are given in Fig. 3c for current efficiency as the response. As can be seen from the figure the $H_2O_2/FeSO_4·7H_2O$ molar ratio did not have a remarkable influence on current efficiency as $FeSO_4·7H_2O$ molar amount and current intensity have. Maximum current efficiency could be obtained at high values of $FeSO_4·7H_2O$ molar amount and low values of current intensity.

According to Eq. (10), current efficiency is proportional to COD removal. Increments in current efficiency with an increase in ferric ion concentration were mainly due to the increase in the in situ generation rate of hydroxyl radical which leads to higher COD removal. Since current efficiency is inversely proportional to the current intensity, and current intensity has a diminished effect on COD removal, a decrease in the current efficiency with increasing current intensity was a predictable outcome.

3.2. Determination of optimal conditions for EF treatment of cheese whey

To achieve the highest treatment performance for EF treatment of cheese whey with the lowest operational cost, the desired goals were simultaneous maximization of COD removal and current efficiency with minimization of energy consumption depending on response surface plots and desirability functions. Obtained optimum operating conditions according to multi-objective optimization through overall multi-desirability function are given in Table 8.

The results imply that maximum organic matter removal and current efficiency along with minimum energy consumption objectives could be accomplished with a high $FeSO_4·7H_2O$ molar amount and $H_2O_2/FeSO_4·7H_2O$ molar ratio under low current intensity conditions. The validity of the predicted response values at optimum operating conditions was controlled by performing an experimental study. Under optimized conditions, model estimations and experimentally observed values of COD removal, energy consumption, and current efficiency are given in Table 9. As seen from the table, obtained COD removal and current efficiency results

Table 7
ANOVA results of current efficiency for EF treatment of cheese whey

Source	*df*	SS_{adj}	MS_{adj}	*F*	*P*	Remark
Model	4	4503.18	1125.80	20.90	≤0.0001	Very significant
x_1	1	444.90	444.90	8.26	0.012	Significant
x_2	1	171.97	171.97	3.19	0.094	Not significant
x_3	1	2704.79	2704.79	50.22	≤0.0001	Very significant
x_3^2	1	1181.52	1181.52	21.94	≤0.0001	Very significant
Error	15	807.90	53.86			
Total	19	5311.08				
R^2 = 0.8479, $R^2_{adjusted}$ = 0.8073, $R^2_{predicted}$ = 0.5242						

Table 8
Optimum operating conditions of EF process

Optimum values			Overall multi-desirability
$FeSO_4·7H_2O$ (mol)	$H_2O_2/FeSO_4·7H_2O$ (mol/mol)	Current intensity (A)	
0.625	14.48	1.22	85.97

Table 9
Model predictions and experimental results at optimum operating conditions

	COD removal (%)	Energy consumption (kWh/kg COD_r)	Current efficiency (%)
Predicted	92.73	0.13	51.37
Observed	86.75	0.36	47.11

indicate conformity to the predicted results by 94% and 91%, respectively whereas energy consumption was underestimated with a difference of 0.25 kWh/kg COD_r between observed value and model prediction. It can be noted that estimated results at optimized conditions for EF treatment of cheese whey were successfully confirmed experimental observations.

4. Conclusion

This research noted the unique and successful application of optimized low-cost graphite-graphite EF to the treatment of cheese whey. In this study, response surface methodology and CCD were employed to obtain significant statistical models indicating linear, interaction and quadratic effects of parameters on responses and to find optimal operating conditions for the EF treatment of cheese whey. In accordance with ANOVA results, high determination coefficient values (R^2 > 80) were acquired for all responses confirming good enough fit of prediction models with experimental data. Under optimized conditions (0.0625 mol $FeSO_4·7H_2O$, 14.48 $H_2O_2/FeSO_4·7H_2O$ molar ratio and 1.22 A current intensity) COD removal, energy consumption and current efficiency were determined as 86.75%, 0.36 kWh/kg COD_r and 47.11%, respectively. In terms of industrial applicability of EF which is a sufficient method for cheese whey treatment, energy consumption reduction in addition to increasing COD removal efficiency is an important criterion. According to the results, it can be concluded that the present treatment with the use of low-cost graphite electrodes yielded highly competitive and promising results under low current density (9.68 mA/cm^2) conditions.

Acknowledgment

This work was supported by Ankara University Scientific Research Projects Coordination Unit [grant number 16B0443001].

Symbols

β_0	–	Constant coefficient
β_j	—	Coefficient of linear effect
β_{ij}	—	Coefficient of quadratic effect
β_{jj}	—	Coefficient of interaction effect
COD_i	—	Initial COD concentration
COD_r	—	COD removed
COD_t	—	Final COD concentration
K_{sp}	—	Solubility product constant
MS_{adj}	—	Adjusted mean squares
S	—	Significant
SS_{adj}	—	Adjusted sum of squares
x	—	Factor
y	—	Response

References

[1] U. Tezcan Un, A. Kandemir, N. Erginel, S.E. Ocal, Continuous electrocoagulation of cheese whey wastewater: an application of response surface methodology, J. Environ. Manage., 146 (2014) 245–250.
[2] R.K. Dereli, F.P. van der Zee, I. Ozturk, J.B. van Lier, Treatment of cheese whey by a cross-flow anaerobic membrane bioreactor: biological and filtration performance, Environ. Res., 168 (2019) 109–117.
[3] G. Güven, A. Perendeci, A. Tanyolaç, Electrochemical treatment of deproteinated whey wastewater and optimization of treatment conditions with response surface methodology, J. Hazard. Mater., 157 (2008) 69–78.
[4] A. Vlyssides, E. Tsimas, E.M. Barampouti, S. Mai, A. Stamatoglou, Implementation of Fenton process on wastewater from a cheese-making factory, Desal. Wat. Treat., 51 (2013) 3069–3075.
[5] A.R. Prazeres, F. Carvalho, J. Rivas, Cheese whey management: a review, J. Environ. Manage., 110 (2012) 48–68.
[6] A.R. Prazeres, J. Rivas, Ú. Paulo, F. Ruas, F. Carvalho, Sustainable treatment of different high-strength cheese whey wastewaters: an innovative approach for atmospheric CO_2 mitigation and fertilizer production, Environ. Sci. Pollut. Res., 23 (2016) 13062–13075.
[7] A. Haridas, S. Suresh, K.R. Chitra, V.B. Manilal, The Buoyant Filter Bioreactor: a high-rate anaerobic reactor for complex wastewater—process dynamics with dairy effluent, Water Res., 39 (2005) 993–1004.
[8] W. Qasim, A.V. Mane, Characterization and treatment of selected food industrial effluents by coagulation and adsorption techniques, Water Resour. Ind., 4 (2013) 1–12.
[9] A. Hamdani, M. Mountadar, O. Assobhei, Comparative study of the efficacy of three coagulants in treating dairy factory waste water, Int. J. Dairy Technol., 58 (2005) 83–88.
[10] A.R. Prazeres, F. Carvalho, J. Rivas, Fenton-like application to pretreated cheese whey wastewater, J. Environ. Manage., 129 (2013) 199–205.
[11] J. Rivas, A.R. Prazeres, F. Carvalho, F. Beltrán, Treatment of cheese whey wastewater: combined coagulation−flocculation and aerobic biodegradation, J. Agric. Food Chem., 58 (2010) 7871–7877.
[12] L. Tirado, Ö. Gökkuş, E. Brillas, I. Sirés, Treatment of cheese whey wastewater by combined electrochemical processes, J. Appl. Electrochem., 48 (2018) 1307–1319.
[13] G. Varank, S.Y. Guvenc, A. Demir, A comparative study of electrocoagulation and electro-Fenton for food industry wastewater treatment: multiple response optimization and cost analysis, Sep. Sci. Technol., 53 (2018) 2727–2740.
[14] P.V. Nidheesh, R. Gandhimathi, Trends in electro-Fenton process for water and wastewater treatment: an overview, Desalination, 299 (2012) 1–15.
[15] J.J. Pignatello, E. Oliveros, A. MacKay, Advanced oxidation processes for organic contaminant destruction based on the fenton reaction and related chemistry, Crit. Rev. Env. Sci. Technol., 36 (2006) 1–84.
[16] P.V. Nidheesh, R. Gandhimathi, Removal of Rhodamine B from aqueous solution using graphite–graphite electro-Fenton system, Desal. Wat. Treat., 52 (2014) 1872–1877.
[17] B. Wang, W.P. Kong, H.Z. Ma, Electrochemical treatment of paper mill wastewater using three-dimensional electrodes with Ti/Co/SnO_2-Sb_2O_5 anode, J. Hazard. Mater., 146 (2007) 295–301.
[18] M. Panizza, M.A. Oturan, Degradation of Alizarin Red by electro-Fenton process using a graphite-felt cathode, Electrochim. Acta, 56 (2011) 7084–7087.
[19] E. Atmaca, Treatment of landfill leachate by using electro-Fenton method, J. Hazard. Mater., 163 (2009) 109–114.

[20] M. Sun, F.Y. Chen, J.H. Qu, H.J. Liu, R.P. Liu, Optimization and control of electro-Fenton process by pH inflection points: a case of treating acrylic fiber manufacturing wastewater, Chem. Eng. J., 269 (2015) 399–407.
[21] E. Brillas, R. Sauleda, J. Casado, Degradation of 4-chlorophenol by anodic oxidation, electro-Fenton, photoelectro-Fenton, and peroxi-coagulation processes, J. Electrochem. Soc., 145 (1998) 759–765.
[22] U. Tezcan Un, A. Kandemir, Treatment of whey wastewater by electrocoagulation and electro-Fenton methods in batch mode, Desal. Wat. Treat., 95 (2018) 88–95.
[23] M. Diagne, N. Oturan, M.A. Oturan, Removal of methyl parathion from water by electrochemically generated Fenton's reagent, Chemosphere, 66 (2007) 841–848.
[24] M. Pimentel, N. Oturan, M. Dezotti, M.A. Oturan, Phenol degradation by advanced electrochemical oxidation process electro-Fenton using a carbon felt cathode, Appl. Catal., B, 83 (2008) 140–149.
[25] E. Brillas, I. Sirés, M.A. Oturan, Electro-Fenton process and related electrochemical technologies based on Fenton's reaction chemistry, Chem. Rev., 109 (2009) 6570–6631.
[26] S. Garcia-Segura, J. Keller, E. Brillas, J. Radjenovic, Removal of organic contaminants from secondary effluent by anodic oxidation with a boron-doped diamond anode as tertiary treatment, J. Hazard. Mater., 283 (2015) 551–557.
[27] O. Ganzenko, N. Oturan, I. Sirés, D. Huguenot, E.D. van Hullebusch, G. Esposito, M.A. Oturan, Fast and complete removal of the 5-fluorouracil drug from water by electro-Fenton oxidation, Environ. Chem. Lett., 16 (2018) 281–286.
[28] D. Rajkumar, J.G. Kim, Oxidation of various reactive dyes with in situ electro-generated active chlorine for textile dyeing industry wastewater treatment, J. Hazard. Mater., 136 (2006) 203–212.
[29] H.Z. Ma, Q.F. Zhuo, B. Wang, Electro-catalytic degradation of methylene blue wastewater assisted by Fe_2O_3-modified kaolin, Chem. Eng. J., 155 (2009) 248–253.
[30] D. Rajkumar, B.J. Song, J.G. Kim, Electrochemical degradation of Reactive Blue 19 in chloride medium for the treatment of textile dyeing wastewater with identification of intermediate compounds, Dyes Pigm., 72 (2007) 1–7.
[31] K. Bensadok, N. El Hanafi, F. Lapicque, Electrochemical treatment of dairy effluent using combined Al and Ti/Pt electrodes system, Desalination, 280 (2011) 244–251.
[32] J.I. Garrote, M. Bao, P. Castro, M.J. Bao, Treatment of tannery effluents by a two step coagulation/flocculation process, Water Res., 29 (1995) 2605–2608.
[33] J. Sarasa, M.P. Roche, M.P. Ormad, E. Gimeno, A. Puig, J.L. Ovelleiro, Treatment of a wastewater resulting from dyes manufacturing with ozone and chemical coagulation, Water Res., 32 (1998) 2721–2727.
[34] J.A. Peres, J. Beltrán de Heredia, J.R. Domínguez, Integrated Fenton's reagent—coagulation/flocculation process for the treatment of cork processing wastewaters, J. Hazard. Mater., 107 (2004) 115–121.
[35] J.M. Duan, X.T. Cao, C. Chen, D.R. Shi, G.M. Li, D. Mulcahy, Effects of $Ca(OH)_2$ assisted aluminum sulfate coagulation on the removal of humic acid and the formation potentials of tri-halomethanes and haloacetic acids in chlorination, J. Environ. Sci., 24 (2012) 1609–1615.
[36] APHA, Standard Methods for the Examination of Water and Wastewater, A.D. Eaton, L.S. Clesceri, E.W. Rice, M.A.H. Franson, Eds., 21st ed., American Public Health Association (APHA), American Water Works Association (AWWA) and the Water Environment Federation (WEF), Washington DC, 2005.
[37] C.L. Lai, S.H. Lin, Treatment of chemical mechanical polishing wastewater by electrocoagulation: system performances and sludge settling characteristics, Chemosphere, 54 (2004) 235–242.
[38] B. Özyurt, Ş. Camcıoğlu, H. Hapoglu, A consecutive electro-coagulation and electro-oxidation treatment for pulp and paper mill wastewater, Desal. Wat. Treat., 93 (2017) 214–228.
[39] S. Camcioglu, B. Ozyurt, H. Hapoglu, Effect of process control on optimization of pulp and paper mill wastewater treatment by electrocoagulation, Process Saf. Environ. Prot., 111 (2017) 300–319.
[40] A.T. Nair, A.R. Makwana, M.M. Ahammed, The use of response surface methodology for modelling and analysis of water and wastewater treatment processes: a review, Water Sci. Technol., 69 (2013) 464–478.
[41] P.V. Nidheesh, R. Gandhimathi, Effect of solution pH on the performance of three electrolytic advanced oxidation processes for the treatment of textile wastewater and sludge characteristics, RSC Adv., 4 (2014) 27946–27954.
[42] D. Hermosilla, M. Cortijo, C.P. Huang, Optimizing the treatment of landfill leachate by conventional Fenton and photo-Fenton processes, Sci. Total Environ., 407 (2009) 3473–3481.
[43] G. Moussavi, M. Aghanejad, The performance of electro-chemical peroxidation process for COD reduction and bio-degradability improvement of the wastewater from a paper recycling plant, Sep. Purif. Technol., 132 (2014) 182–186.
[44] K. Thirugnanasambandham, V. Sivakumar, Modeling and optimization of advanced oxidation treatment of beer industry wastewater using electro-Fenton process, Environ. Prog. Sustainable Energy, 34 (2015) 1072–1079.
[45] M.F. Sevimli, E. Deliktaş, S. Şahinkaya, D. Güçlü, A comparative study for treatment of white liquor by different applications of Fenton process, Arabian J. Chem., 7 (2014) 1116–1123.
[46] N. Jaafarzadeh, F. Ghanbari, M. Ahmadi, M. Omidinasab, Efficient integrated processes for pulp and paper wastewater treatment and phytotoxicity reduction: permanganate, electro-Fenton and Co_3O_4/UV/peroxymonosulfate, Chem. Eng. J., 308 (2017) 142–150.